

NV-Center Quantum Sensing for Biomedicine: Simulated Nanodiamond Relaxometry

Van Tien Nguyen

Department of Electrical Engineering
The University of Texas at San Antonio
San Antonio, TX, USA
tien.nguyen@utsa.edu

Abstract—Quantum sensors based on nitrogen–vacancy (NV) centers in diamond combine atomic-scale sensing with operation at room temperature, and are now being explored from organ-level magnetoencephalography to subcellular biophysics. In this project, we give a concise overview of NV-based quantum sensing in biomedicine and then develop a compact numerical case study inspired by recent experiments on NV-nanodiamond relaxometry of mitochondrial free radicals. We first summarize three main NV modalities—wide-field NV magnetometry, nano-/microscale NV-NMR, and NV nanodiamond thermometry—and highlight how they collectively cover length scales from tissues down to organelles. We then focus on the work of Nie et al., where fluorescent NV-doped nanodiamonds targeted to mitochondria report on local radical production via changes in the NV longitudinal relaxation time T_1 . We model each nanodiamond as an effective qubit undergoing amplitude damping and implement an inversion-recovery protocol. For three representative relaxation times $T_1 = \{3.0, 1.5, 0.7\}$ ms that mimic low, medium, and high radical concentrations, single-exponential fits recover the underlying T_1 values with relative errors below 0.2% using 4096 shots, reproducing the qualitative separation between control and stressed conditions. Extending the model to homogeneous ensembles of N_{NV} independent NV centers, we show that the standard deviation of the estimated T_1 scales approximately as $1/\sqrt{N_{\text{NV}}}$, consistent with the standard quantum limit for independent sensors. The simulation framework provides an instructive bridge between the quantum-sensing literature and code-based exploration of biomedical NV sensing.

Index Terms—quantum sensing, nitrogen–vacancy center, fluorescent nanodiamond, relaxometry, free radicals, mitochondria, biophotonics

I. Introduction

Biomedical science demands tools that can probe physiology from organs and tissues down to single cells and organelles. Classical platforms such as SQUID-based magnetoencephalography (MEG), fluorescence microscopy, and bulk nuclear magnetic resonance (NMR) have enabled major advances, but each faces trade-offs between sensitivity, spatial resolution, invasiveness, and experimental overhead. For example, SQUID-MEG requires cryogenic cooling and provides millimeter–centimeter resolution at the whole-brain scale, whereas optical fluorescence can achieve subcellular resolution but often relies on labels that bleach, blink, or perturb the biology they report.

Quantum sensing offers an alternative route by exploiting coherence and interference in engineered quantum

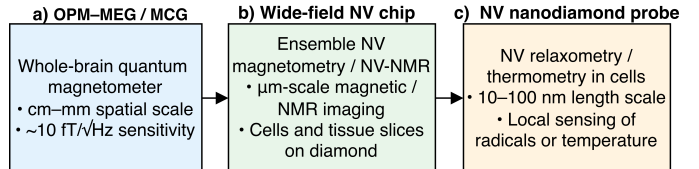


Fig. 1. Quantum sensors for biomedicine across spatial scales: (a) organ-scale OPM magnetometry, (b) tissue-/cell-scale ensemble NV sensing, and (c) subcellular NV nanodiamond sensing.

systems to estimate external fields with high sensitivity at small length scales [1]. Among the available platforms, two have become particularly relevant in biomedicine. Optically pumped magnetometers (OPMs) based on alkali-vapor cells have enabled wearable MEG and magneto-cardiography at room temperature [2]. Solid-state defects in diamond, especially the negatively charged nitrogen–vacancy (NV^-) center, support room-temperature optical initialization and readout, long coherence times, and nanometer proximity to biological samples [3], [4].

NV centers now underpin three main biomedical sensing modalities: wide-field NV magnetometry of cells and tissues, nano- and microscale NV-detected NMR, and NV-based thermometry with nanodiamonds [1], [4]. Together they span organ-, tissue-, and subcellular length scales. Within this landscape, NV-nanodiamond relaxometry has recently emerged as a powerful probe of free radicals and redox biology at the organelle level [5]–[7]. In particular, Nie et al. used mitochondria-targeted fluorescent nanodiamonds (FNDs) to monitor metabolic activity in single mitochondria via changes in the NV longitudinal relaxation time T_1 [8].

The goals of this report are twofold. First, we give a compact survey of NV-based quantum sensors in biomedicine, emphasizing how the three NV modalities complement OPMs across spatial scales. Second, we select NV-nanodiamond T_1 relaxometry of mitochondrial radicals as a concrete case study and implement a simplified numerical model in Qiskit that captures its core sensing principle. The resulting framework is suitable both for conceptual understanding and for future extensions in more detailed simulations.

II. NV-Based Quantum Sensors in Biomedicine

A. Quantum Sensors and OPMs

A quantum sensor is a quantum system (or ensemble) whose state responds coherently to an external parameter such as magnetic field, electric field, or temperature [1]. In biomedicine, the most mature macroscopic platform is the alkali-vapor OPM, where spin-polarized atomic ensembles detect femtotesla-level magnetic fields at room temperature [4]. OPM-based MEG has demonstrated sensor arrays integrated into lightweight helmets that closely follow the head shape and allow moderate head motion, enabling more naturalistic experiments than conventional SQUID-MEG [2]. However, OPMs remain limited to millimeter-centimeter spatial resolution and cannot directly access cellular and subcellular processes.

B. NV-Center Modalities Across Scales

The NV center consists of a substitutional nitrogen adjacent to a carbon vacancy, forming a spin-1 electronic ground state that can be optically initialized and read out at room temperature [3]. In most sensing protocols, the $|m_s = 0\rangle$ and $|m_s = -1\rangle$ sublevels are treated as an effective qubit addressed by microwave fields. Depending on geometry and readout, three main modalities have crystallized [1], [4]:

- Wide-field NV magnetometry: A diamond chip with a near-surface NV layer is imaged by a wide-field fluorescence microscope. Cells, tissue slices, or small organisms are placed on the surface, and the NV fluorescence encodes 2D maps of the magnetic field $B(x, y)$ from neuronal currents, ferritin, or magnetic nanoparticle labels [9]–[11].
- Nano-/microscale NV-NMR: Near-surface NV centers detect nuclear-spin precession in nanoscale or microfluidic samples via dynamical decoupling sequences. Experiments have demonstrated NMR spectroscopy of $(5 \text{ nm})^3$ volumes and picoliter droplets with high spectral resolution [12]–[14].
- NV thermometry with nanodiamonds: NV-doped nanodiamonds (typically 50–100 nm) are internalized in cells or small organisms. Temperature-dependent shifts of the zero-field splitting $D(T)$ are read out optically, enabling subcellular temperature mapping and *in vivo* thermogenesis measurements [15]–[17].

Figure 1 illustrates how OPMs and NV-based sensors jointly cover organ-, tissue-, and subcellular scales.

III. NV-Nanodiamond Relaxometry of Free Radicals

A. Physical Principle of NV T_1 Relaxometry

The NV ground state is described (in a simplified form) by

$$\hat{H} = D(T)\hat{S}_z^2 + \gamma_e \mathbf{B} \cdot \hat{\mathbf{S}} + \hat{H}_{\text{env}}, \quad (1)$$

where $D(T)$ is the zero-field splitting, $\gamma_e/2\pi \approx 28 \text{ GHz/T}$ is the electron gyromagnetic ratio, \mathbf{B} is a bias field, and \hat{H}_{env} accounts for coupling to environmental spins [1],

[3]. Restricting to the $\{|0\rangle, |-1\rangle\}$ subspace and working at fixed bias, the longitudinal relaxation time T_1 is set by transverse magnetic-field noise at the NV transition frequency [5], [6].

Paramagnetic species such as free radicals generate additional magnetic noise in the MHz–GHz range, which increases the NV relaxation rate. For a fixed chemical environment, it is convenient to describe the dependence on the local radical concentration c_{rad} phenomenologically as

$$\frac{1}{T_1} \approx \frac{1}{T_1^{(0)}} + k c_{\text{rad}}, \quad (2)$$

where $T_1^{(0)}$ is the intrinsic relaxation time in the absence of radicals and k is an effective coupling coefficient that depends on the radical species and distance distribution [6], [7]. Changes in metabolic activity that modify radical production thus appear as shifts in T_1 .

Experimentally, T_1 is measured via optical relaxometry: the NV ensemble is polarized into $|0\rangle$ by a green laser pulse, allowed to relax in the dark for a variable delay τ , and read out optically. Conceptually, this protocol is equivalent to preparing $|1\rangle$, waiting time τ , and measuring the excited-state population

$$P_1(\tau) = P_1^{\text{eq}} + (P_1(0) - P_1^{\text{eq}}) e^{-\tau/T_1}, \quad (3)$$

so that single-exponential fits to the fluorescence contrast versus τ yield T_1 .

B. Summary of Nie et al.

Nie et al. implemented this scheme using $\sim 70 \text{ nm}$ fluorescent nanodiamonds containing ensembles of NV centers [8]. After surface oxidation, the nanodiamonds were coated with polyethylene glycol and anti-VDAC2 antibodies (aVDAC2-FNDs), which bind to voltage-dependent anion channel 2 on the outer mitochondrial membrane. Confocal imaging with MitoTracker confirmed that aVDAC2-FNDs colocalized with mitochondria, whereas unmodified FNDs remained in the cytosol.

Using a home-built confocal microscope and pulsed 532 nm excitation, the authors performed T_1 measurements on single FNDs in live macrophage cells by varying the dark time τ and recording NV photoluminescence. Mitochondria-targeted FNDs exhibited systematically shorter T_1 than cytosolic FNDs, consistent with enhanced radical production at mitochondria. Chemical perturbations with CCCP (an uncoupler) and antioxidant enzymes (SOD+CAT) produced predictable shifts of T_1 , and control experiments supported the interpretation that the dominant signal is due to free radicals rather than confounding factors [6], [8], [18], [19]. Overall, these results establish NV-nanodiamond T_1 relaxometry as a quantitative, non-bleaching probe of subcellular redox biology.

IV. Numerical Study in Qiskit

We now implement a minimal model of NV-nanodiamond T_1 relaxometry in Qiskit. Since no NV

biophotonics setup is available, all results are obtained from quantum-circuit simulations calibrated to be qualitatively consistent with Refs. [6], [8], [18]. The aims are (i) to reproduce the separation of T_1 values between low and high radical conditions, and (ii) to quantify how the precision of T_1 estimation improves with the number of NV centers in a homogeneous ensemble.

A. Simulation Model

Unless stated otherwise, each nanodiamond is modeled as a single effective spin- $\frac{1}{2}$ with computational basis $\{|0\rangle, |1\rangle\} \equiv \{|m_s=0\rangle, |m_s=-1\rangle\}$. Longitudinal relaxation during a dark interval of duration τ is modeled as an amplitude-damping channel with damping probability

$$p(\tau) = 1 - \exp(-\tau/T_1), \quad (4)$$

so that an initially inverted state has excited-state population $P_1(\tau) = \exp(-\tau/T_1)$, consistent with Eq. (3).

To mimic the relative T_1 values observed in mitochondria-targeted nanodiamonds under control and stressed conditions [8], we choose three representative relaxation times

$$T_1^{(\text{low})} = 3.0 \text{ ms}, T_1^{(\text{med})} = 1.5 \text{ ms}, T_1^{(\text{high})} = 0.7 \text{ ms}, \quad (5)$$

corresponding to low, medium, and high effective radical concentrations. For each condition we sample $M = 25$ delay times τ_i uniformly in $[0, \tau_{\max}]$ with $\tau_{\max} = 9$ ms, and estimate $P_1(\tau_i)$ from $N_{\text{shots}} = 4096$ circuit repetitions.

B. Single-NV Relaxometry

For a single NV center (one qubit), the inversion-recovery sequence at each delay consists of: (i) initialize in $|0\rangle$, (ii) apply an X gate to prepare $|1\rangle$, (iii) apply an identity gate subject to amplitude-damping noise with parameter $p(\tau_i)$, and (iv) measure in the computational basis. To characterize shot noise, for each condition we repeat the full set of delay times 20 times, generating 20 independent noisy inversion-recovery curves.

For each run, the samples $P_1(\tau_i)$ are fit with the single-exponential model

$$P_1(\tau) \approx A \exp(-\tau/T_1) + C, \quad (6)$$

with T_1 , A , and C treated as free parameters and optimized via nonlinear least squares (`scipy.optimize.curve_fit`). We then compute the sample mean and standard deviation of the fitted relaxation time \hat{T}_1 over the 20 runs.

Figure 2 shows the mean simulated data and best-fit curves for the three conditions. As in Nie et al. [8], increasing radical concentration shortens T_1 and yields visibly faster decay. Table I reports the true relaxation times together with the mean fitted values and their relative errors. The mean estimates are unbiased at the sub-percent level, with relative errors below 0.2% in all three cases, confirming that a simple single-exponential model suffices to recover T_1 with high accuracy at realistic shot counts.

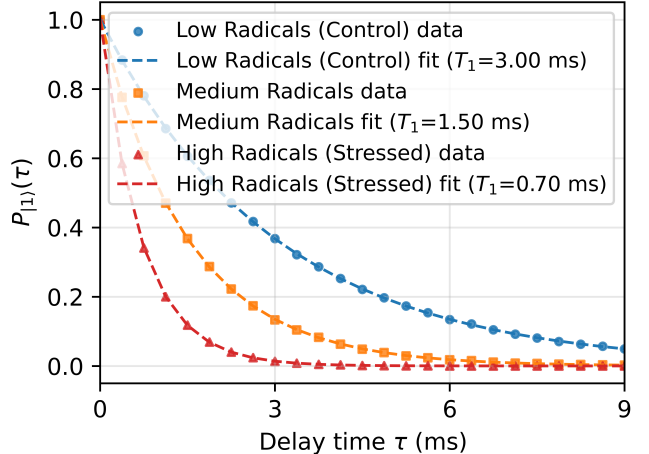


Fig. 2. Simulated inversion-recovery curves for a single NV center under three effective radical concentrations. Markers: Qiskit data (averaged over 20 simulation runs). Lines: single-exponential fits. Shorter T_1 (high-radical case) leads to a markedly faster decay, in qualitative agreement with mitochondria-targeted nanodiamond experiments [8].

TABLE I

True and mean fitted relaxation times for three simulated single-NV conditions, based on 20 independent Qiskit runs per condition.

Condition	True T_1 (ms)	Mean \hat{T}_1 (ms)	Rel. error (%)
Low radicals (control)	3.00	2.995	-0.16
Medium radicals	1.50	1.498	-0.13
High radicals (stressed)	0.70	0.699	-0.10

C. Ensemble NV Sensors and SQL Scaling

To study how multiple NV centers per nanodiamond can improve sensitivity, we next model a homogeneous ensemble of N_{NV} independent NV centers as N_{NV} qubits. Each qubit undergoes the same amplitude-damping channel with $T_1 = T_1^{(\text{med})} = 1.5$ ms. For each dark time τ_i we prepare $|1\rangle^{\otimes N_{\text{NV}}}$, apply the noisy identity on all qubits, and measure all in the computational basis. The quantity of interest is the average excited-state population per NV, obtained by averaging over all qubits and $N_{\text{shots}} = 2048$ repetitions.

For each $N_{\text{NV}} \in \{1, 2, 4, 8\}$ we repeat the full simulated experiment 20 times and fit T_1 as above, obtaining a sample mean $\mathbb{E}[\hat{T}_1]$ and standard deviation $\text{std}(\hat{T}_1)$. The numerical results are summarized in Table II. The means remain essentially unbiased (all within $\approx 0.2\%$ of 1.5 ms), while the standard deviation decreases systematically with ensemble size.

Figure 3 plots $\text{std}(\hat{T}_1)$ versus N_{NV} on log-log scales together with a reference line proportional to $1/\sqrt{N_{\text{NV}}}$. The close agreement confirms that, in the independent-sensor regime relevant for current NV-nanodiamond relaxometry [6], [8], the precision of T_1 estimation improves

TABLE II

Estimated relaxation times for homogeneous NV ensembles with $T_1^{(\text{med})} = 1.5$ ms, obtained from 20 independent Qiskit simulations per ensemble size.

N_{NV}	Mean \hat{T}_1 (ms)	$\text{std}(\hat{T}_1)$ (ms)	Rel. std (%)
1	1.500	0.018	1.2
2	1.499	0.017	1.1
4	1.497	0.008	0.6
8	1.500	0.006	0.4

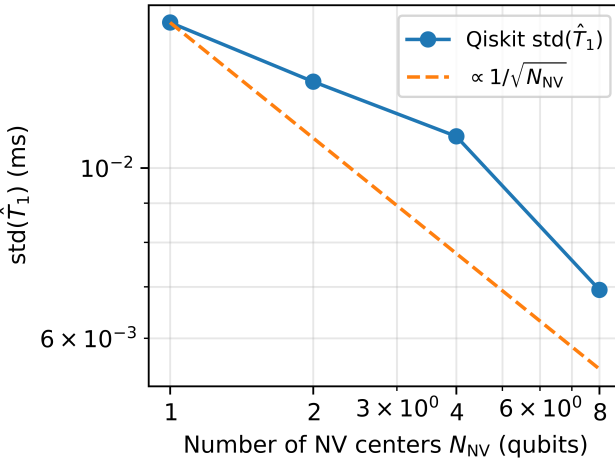


Fig. 3. Standard-quantum-limit behavior of homogeneous NV ensembles in Qiskit. Blue: empirical standard deviation of the fitted relaxation time \hat{T}_1 as the number of NV centers N_{NV} is increased from 1 to 8. Orange dashed: reference line $\propto 1/\sqrt{N_{\text{NV}}}$.

at the standard quantum limit rather than exhibiting Heisenberg scaling.

V. Conclusion

We have examined how NV-center quantum sensors can be applied to biomedicine by combining a compact survey with a simulation-based case study. On the survey side, we reviewed how OPMs and NV-based modalities—wide-field NV magnetometry, nano-/microscale NV-NMR, and NV nanodiamond thermometry—collectively span organo-to organelle-level length scales and enable measurements ranging from single-neuron action potentials to picoliter NMR spectroscopy and subcellular thermogenesis [11], [14], [16], [17].

Motivated by recent experiments on NV-nanodiamond relaxometry of mitochondrial free radicals [8], we developed a simplified Qiskit model in which each nanodiamond is represented as a single qubit subject to amplitude damping with relaxation time T_1 . Using an inversion-recovery protocol, we showed that single-exponential fits can reliably recover three representative T_1 values corresponding to low, medium, and high radical concentrations with sub-percent relative error at realistic shot counts. Extending the model to homogeneous ensembles of NV

centers, we observed that the standard deviation of the fitted T_1 scales as $1/\sqrt{N_{\text{NV}}}$, consistent with standard-quantum-limit behavior for independent sensors.

The model intentionally neglects multi-exponential relaxation, spatial inhomogeneity within nanodiamonds, and detailed radical diffusion, but it provides a clear starting point for more realistic studies. Future work could incorporate distributed T_1 values, more complex noise spectra, or coupling to microscopic models of radical dynamics, and could explore hybrid protocols that combine T_1 relaxometry with NV-NMR or thermometry. From a pedagogical perspective, the project illustrates how quantum-sensing concepts in the literature can be translated into concrete, reproducible simulations in a quantum-computing framework.

References

- [1] C. L. Degen, F. Reinhard, and P. Cappellaro, “Quantum sensing,” Rev. Mod. Phys., vol. 89, p. 035002, Jul 2017. [Online]. Available: <https://link.aps.org/doi/10.1103/RevModPhys.89.035002>
- [2] E. Boto, N. Holmes, J. Leggett, G. Roberts, V. Shah, S. S. Meyer, L. D. Muñoz, K. J. Mullinger, T. M. Tierney, S. Bestmann, G. R. Barnes, R. Bowtell, and M. J. Brookes, “Moving magnetoencephalography towards real-world applications with a wearable system,” Nature, vol. 555, no. 7698, pp. 657–661, Mar. 2018.
- [3] R. Schirhagl, K. Chang, M. Loretz, and C. L. Degen, “Nitrogen-vacancy centers in diamond: Nanoscale sensors for physics and biology,” Annual Review of Physical Chemistry, vol. 65, no. Volume 65, 2014, pp. 83–105, 2014. [Online]. Available: <https://www.annualreviews.org/content/journals/10.1146/annurev-physchem-040513-103659>
- [4] N. Aslam, H. Zhou, E. K. Urbach, M. J. Turner, R. L. Walsworth, M. D. Lukin, and H. Park, “Quantum sensors for biomedical applications,” Nature Reviews Physics, vol. 5, no. 3, pp. 157–169, Mar. 2023.
- [5] J.-P. Tetienne, T. Hingant, L. Rondin, A. Cavaillès, L. Mayer, G. Dantelle, T. Gacoin, J. Wrachtrup, J.-F. Roch, and V. Jacques, “Spin relaxometry of single nitrogen-vacancy defects in diamond nanocrystals for magnetic noise sensing,” Phys. Rev. B, vol. 87, p. 235436, Jun 2013. [Online]. Available: <https://link.aps.org/doi/10.1103/PhysRevB.87.235436>
- [6] A. Mzyk, A. Sigaeva, and R. Schirhagl, “Relaxometry with nitrogen vacancy (NV) centers in diamond,” Acc. Chem. Res., vol. 55, no. 24, pp. 3572–3580, Dec. 2022.
- [7] Y. Wu and T. Weil, “Recent developments of nanodiamond quantum sensors for biological applications,” Adv Sci (Weinh), vol. 9, no. 19, p. e2200059, Mar. 2022.
- [8] L. Nie, A. C. Nusantara, V. G. Damle, R. Sharmin, E. P. P. Evans, S. R. Hemelaar, K. J. van der Laan, R. Li, F. P. P. Martinez, T. Vedelaar, M. Chipaux, and R. Schirhagl, “Quantum monitoring of cellular metabolic activities in single mitochondria,” Science Advances, vol. 7, no. 21, p. eabf0573, 2021. [Online]. Available: <https://www.science.org/doi/abs/10.1126/sciadv.abf0573>
- [9] D. Le Sage, K. Arai, D. R. Glenn, S. J. DeVience, L. M. Pham, L. Rahn-Lee, M. D. Lukin, A. Yacoby, A. Komeili, and R. L. Walsworth, “Optical magnetic imaging of living cells,” Nature, vol. 496, no. 7446, pp. 486–489, Apr. 2013.
- [10] D. R. Glenn, K. Lee, H. Park, R. Weissleder, A. Yacoby, M. D. Lukin, H. Lee, R. L. Walsworth, and C. B. Connolly, “Single-cell magnetic imaging using a quantum diamond microscope,” Nature Methods, vol. 12, no. 8, pp. 736–738, Aug. 2015.
- [11] J. F. Barry, M. J. Turner, J. M. Schloss, D. R. Glenn, Y. Song, M. D. Lukin, H. Park, and R. L. Walsworth, “Optical magnetic detection of single-neuron action potentials using quantum defects in diamond,” Proceedings of the National Academy of Sciences, vol. 113, no. 49, pp. 14133–14138,

2016. [Online]. Available: <https://www.pnas.org/doi/abs/10.1073/pnas.1601513113>
- [12] T. Staudacher, F. Shi, S. Pezzagna, J. Meijer, J. Du, C. A. Meriles, F. Reinhard, and J. Wrachtrup, “Nuclear magnetic resonance spectroscopy on a (5-nanometer)³ sample volume,” *Science*, vol. 339, no. 6119, pp. 561–563, Feb. 2013.
- [13] N. Aslam, M. Pfender, P. Neumann, R. Reuter, A. Zappe, F. F. de Oliveira, A. Denisenko, H. Sumiya, S. Onoda, J. Isoya, and J. Wrachtrup, “Nanoscale nuclear magnetic resonance with chemical resolution,” *Science*, vol. 357, no. 6346, pp. 67–71, 2017. [Online]. Available: <https://www.science.org/doi/abs/10.1126/science.aam8697>
- [14] D. R. Glenn, D. B. Bucher, J. Lee, M. D. Lukin, H. Park, and R. L. Walsworth, “High-resolution magnetic resonance spectroscopy using a solid-state spin sensor,” *Nature*, vol. 555, no. 7696, pp. 351–354, Mar. 2018.
- [15] V. M. Acosta, E. Bauch, M. P. Ledbetter, A. Waxman, L.-S. Bouchard, and D. Budker, “Temperature dependence of the nitrogen-vacancy magnetic resonance in diamond,” *Phys. Rev. Lett.*, vol. 104, p. 070801, Feb 2010. [Online]. Available: <https://link.aps.org/doi/10.1103/PhysRevLett.104.070801>
- [16] G. Kucsko, P. C. Maurer, N. Y. Yao, M. Kubo, H. J. Noh, P. K. Lo, H. Park, and M. D. Lukin, “Nanometre-scale thermometry in a living cell,” *Nature*, vol. 500, no. 7460, pp. 54–58, Aug. 2013.
- [17] M. Fujiwara, S. Sun, A. Dohms, Y. Nishimura, K. Suto, Y. Takezawa, K. Oshimi, L. Zhao, N. Sadzak, Y. Umehara, Y. Teki, N. Komatsu, O. Benson, Y. Shikano, and E. Kage-Nakadai, “Real-time nanodiamond thermometry probing in vivo thermogenic responses,” *Science Advances*, vol. 6, no. 37, p. eaba9636, 2020. [Online]. Available: <https://www.science.org/doi/abs/10.1126/sciadv.aba9636>
- [18] L. Nie, A. C. Nusantara, V. G. Damle, M. V. Baranov, M. Chipaux, C. Reyes-San-Martin, T. Hamoh, C. P. Epperla, M. Guricova, P. Cigler, G. van den Bogaart, and R. Schirhagl, “Quantum sensing of free radicals in primary human dendritic cells,” *Nano Lett.*, vol. 22, no. 4, pp. 1818–1825, Feb. 2022.
- [19] R. Sharmin, T. Hamoh, A. Sigaeva, A. Mzyk, V. G. Damle, A. Morita, T. Vedelaar, and R. Schirhagl, “Fluorescent nanodiamonds for detecting Free-Radical generation in real time during shear stress in human umbilical vein endothelial cells,” *ACS Sens.*, vol. 6, no. 12, pp. 4349–4359, Dec. 2021.